International Journal of Nanomedicine

Dovepress
open access to scientific and medical research

Open Access Full Text Article

ORIGINAL RESEARCH

Fabrication Of Dual pH/redox-Responsive Lipid-Polymer Hybrid Nanoparticles For Anticancer Drug Delivery And Controlled Release

This article was published in the following Dove Press journal:
International Journal of Nanomedicine

Wanfu Men[1]
Peiyao Zhu[1]
Siyuan Dong[1]
Wenke Liu[1]
Kun Zhou[1]
Yu Bai[1]
Xiangli Liu[1]
Shulei Gong[1]
Can Yang Zhang[2]
Shuguang Zhang[1]

[1]Department of Thoracic Surgery, The First Affiliated Hospital of China Medical University, Shenyang 110001, People's Republic of China; [2]Department of Pharmaceutical Sciences, College of Pharmacy and Pharmaceutical Sciences, Washington State University, Spokane, WA 99210, USA

Background: The development of biocompatible nanocarriers that can efficiently encapsulate and deliver anticancer drug to the tumor site and provide controlled release of cargos in response to the specific cues for cancer therapy is of great significance.

Methods: In this work, dual pH/redox-responsive fabrication of hybrid lipid-polymer nanoparticles (LPNPs) self-assembled from amphiphilic polymer poly(ethylene glycol) methyl ether-grafted disulfide-poly(*β*-amino esters) (PBAE-ss-mPEG) and PEGylated lipid were prepared and used as drug delivery carriers. The optimization of PEGylated lipid modification was confirmed by analysis of particle size, polydispersity index (PDI), cellular uptake, serum stability, and drug loading capacity. The pK_b value of LPNPs was determined as 6.55, indicating the pH-sensitivity. The critical micelle concentration (CMC) values and zeta-potential of LPNPs at different pH values were investigated to confirm its pH-sensitivity. The morphology of LPNPs before and after incubation with reducing agent was imaged to study the redox-responsibility.

Results: The in vitro results showed that the drug had controlled release from LPNPs triggered by low pH and high concentration of reducing agent. Furthermore, the cytotoxicity of LPNPs was very low, and the doxorubicin (DOX)-loaded LPNPs could efficiently induce the death of tumor cells in comparison to free DOX.

Conclusion: All results demonstrated that the fabricated LPNPs could be potential anticancer drug delivery carriers with a pH/redox-triggered drug release profile, and PEGylated lipid modification might be a useful method to fabricate the drug delivery platform.

Keywords: pH-sensitive, redox-sensitive, lipid-polymer, hybrid, drug delivery, anticancer, stimuli-responsiveness

Correspondence: Shuguang Zhang
Department of Thoracic Surgery, The First Affiliated Hospital of China Medical University, No. 155 North Nanjing Street, Heping District, Shenyang 110001, Liaoning Province, People's Republic of China
Tel +86 13909886618
Email shgzhang@cmu.edu.cn

Can Yang Zhang
Singapore-MIT Alliance for Research and Technology, 1 Create Way, #03-12/13/14 Enterprise Wing, Singapore 138602, Singapore
Tel +65 9499 0710
Email canyang.zhang@smart.mit.edu

Introduction

Cancer is still a leading cause of death worldwide.[1] In the past decades, a variety of therapeutic strategies for cancer treatment have been developed including gene therapy,[2] photodynamic therapy (PDT),[3] photothermal therapy (PTT),[4] and immunotherapy,[5] etc., but the chemotherapy is still the most common and effective way to treat cancer in clinic.[6] Unfortunately, the existing barriers significantly limit the effectiveness of anticancer drugs (eg, doxorubicin, paclitaxel, camptothecin, and *cis*-platinum) in clinic use, including quick clearance by reticuloendothelial system (RES) and poor solubility, leading to low therapeutic efficacy.[7–10] Furthermore, the traditional anticancer drug is not able to distinguish tumor cells from the healthy tissue cells, suggesting non-specific killing that leads to severe side-effects such as

submit your manuscript | www.dovepress.com
DovePress
http://doi.org/10.2147/IJN.S226798

cardiotoxicity and organ dysfunction.[11] To overcome these obstacles, drug delivery systems (DDSs)-based nanomedicine has attracted more and more attention with rapid development of nanotechnology in these years.[12,13] For instance, Zhang et al[14] prepared intelligent pH-sensitive polymeric micelles (PMs) which were self-assembled from cholesterol-grafted PEGylated peptides. The PMs showed high drug loading capacity and were able to accumulate at the tumor site due to enhanced permeability and retention (EPR) effects with reduced side-effects. Wang et al[15] reported the development of a functional liposome constructed by incorporating a small proportion of porphyrin (pyropheophorbide) conjugated lipid. This liposome could efficiently deliver doxorubicin to the site of tumor and control release the cargos on demand.

As reported, the tumor microenvironment (TME) exhibited special features compared to the normal condition, such as low pH value due to elevated levels of lactic acid caused by poor oxygen perfusion and high levels of glutathione (GSH) with a higher intracellular concentration (1–11 mM) than extracellular (0.01 mM) spaces.[7,16–18] These distinguishing properties have been thoroughly investigated and widely used as specific cues for targeted drug delivery and controlled release. For example, Zhang et al[19] designed and prepared a dual pH/redox-responsive drug delivery system (DA-ss-NPs) for co-delivery of all-trans-retinoic acid (ATRA) and paclitaxel (PTX) to improve the therapeutic efficacy. Xu et al[20] reported a dual pH/redox-responsive triptolide (TRI)-loaded nanoparticles constructed by conjugating DOX molecules on the side of poly(ethylene glycol)-*b*-poly(L-lysine) (PEG-*b*-PLL) through disulfides and 2,3-dimethylmaleic anhydride (DMA) which showed pH and GSH-triggered drug release profile and improved antitumor effect.

Inspired by the specific properties in TME, we designed and prepared dual pH and redox-responsive hybrid lipid-polymer nanoparticles (LPNPs) for anticancer drug delivery and controlled release in the present work. The LPNPs were fabricated with the PEGylated lipid (DSPE-mPEG) and amphiphilic copolymer poly(ethylene glycol) methyl ether-grafted disulfide-poly(*β*-amino esters) (PBAE-ss-mPEG).[21] PBAE has been thoroughly studied and extensively used as pH-sensitive polymer for anticancer drug and therapeutic gene delivery in these decades.[22–26] Disulfide bonds are able to be cleavage by responding to the high GSH concentration.[27] The hydrophilic mPEG segment is nonimmunogenic, nonantigenic, and nontoxic, which is generally used to prepare biocompatible nanoparticles.[28–30] As reported, the PEGylated lipid could facilitate the uptake and internalization of NPs by cells through endocytosis.[31] The DSPE segment forms the core of the nanoparticle, thereby providing the drug loading space.[32] The PBAE segment forms the pH-sensitive middle layer which could enhance the drug loading capacity.[33] The PEG segment forms the hydrophilic shell and surrounds on the surface of the nanoparticle which provides a compact and negative charged outerwear to maintain the stability for prolonged circulation time.[34] Figure 1 shows the fabrication of LPNPs and pH/redox-triggered drug release profiles. Moreover, the physicochemical properties of LPNPs, including particle size, zeta-potential, cytotoxicity, etc. will be investigated in this work.

Materials And Methods

Materials

Poly(ethylene glycol) methyl ether-grafted disulfide-poly (*β*-amino esters) ($PBAE_{3100}$-ss-$mPEG_{2000}$) was synthesized as reported in our previous work.[21] Doxorubicin hydrochloride (DOX-HCl) was purchased from Wuhan Yuan Cheng Gong Chuang Co. Ltd (Wuhan, China). 1,2-distearoyl-*sn*-glycero-3-phosphoethanolamine-N-[methyl ether (polyethylene glycol)] (DSPE-mPEG, M_w= 2000) was purchased from Laysan Bio Inc. Triethylamine (TEA, > 99%), pyrene (99%), DL-dithiothreitol (DTT), dichloromethane (DCM), dimethyl sulfoxide (DMSO), chloroform, and all other chemical reagents (Sigma-Aldrich) were used as received. CCK-8 kits were purchased from Sigma-Aldrich. Dulbecco's modified eagle medium (DMEM) growth media, fetal bovine serum (FBS), phosphate buffered saline (PBS), trypsin, penicillin, and streptomycin were all purchased from Invitrogen. Lewis lung carcinoma (3LL) cells were obtained from the American Type Culture Collection (ATCC), and all other reagents were used as received.

Preparation Of Blank And DOX-Loaded NPs

For the preparation of blank PMs and DOX-loaded PMs without DSPE-mPEG modification, DOX-HCl (0, 10 mg, 15 mg, 25 mg) was dissolved into DMF, followed by dropwise addition of TEA (10 μL per 10 mg drug) to remove hydrochloride with gentle stirring at room temperature. After 1 hour, 50 mg PBAE-ss-mPEG was added with stirring. The mixed solution was transferred into a cellulose membrane bag (MWCO 3500–4000 Da) and immersed into deionized water (1 L) for dialysis at room

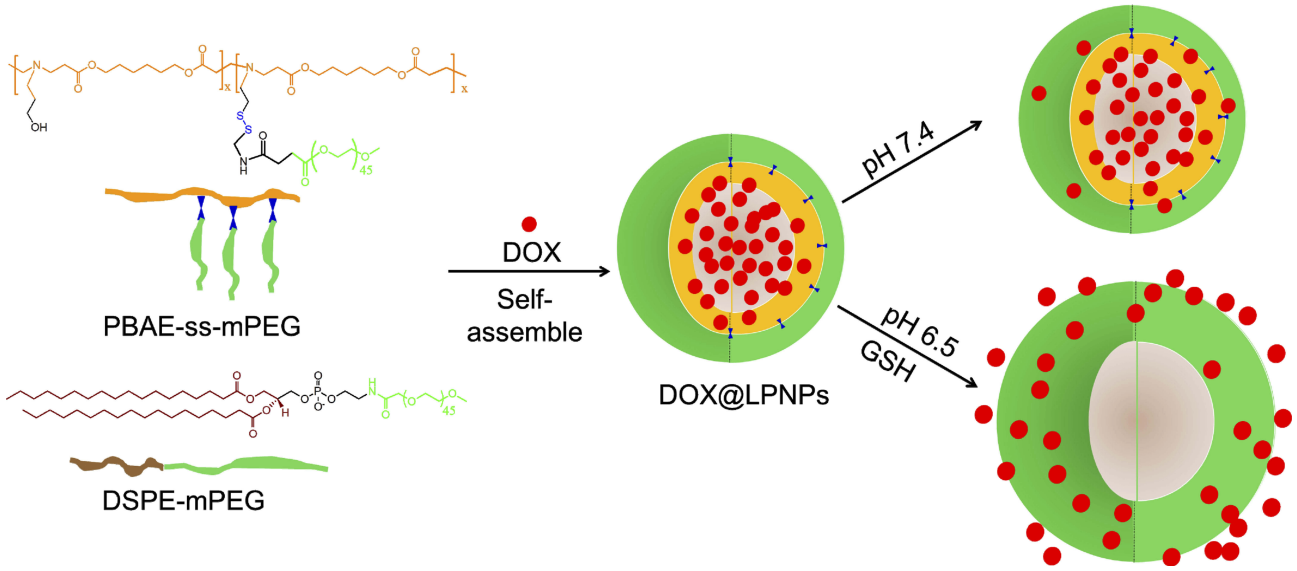

Figure 1 Schematic illustration of self-assembly of hybrid lipid-polymer nanoparticles (LPNPs) loading anticancer drug DOX and controlled release profile triggered by pH and reducing agent.

temperature. The deionized water was replaced every 2 hours in the first 12 hours, and every 6 hours in the next 36 hours. The resulting solution was filtered by a 0.45 μm filter. After lyophilization, the blank and DOX-loaded PMs were obtained and stored at −20°C.

For the preparation of blank LPNPs and DOX-loaded LPNPs with DSPE-mPEG modification, 15 mg DOX-HCl was dissolved into DMF and treated with TEA as aforementioned. Then 50 mg mixed polymers at different mole ratios (PBAE-ss-mPEG: DSPE-mPEG=100:0, 97:3, 95:5, 93:7 and 90:10) were added with stirring. The mixed solution was moved into a cellulose membrane bag (MWCO 3,500–4,000 Da) and dialyzed against deionized water (1 L) for 48 hours. After filtration and lyophilization, the blank LPNPs and DOX-loaded LPNPs were obtained and stored at −20°C for further study.

Confirmation Of Drug Loading Capacity

The drug loading content (LC) and encapsulation efficiency (EE) of PMs and LPNPs with different amounts of PEGylated lipid were measured by a UV-vis spectrophotometer (UV-2450, Shimadzu, Japan). In brief, 1 mg of DOX-loaded PMs or DOX-loaded LPNPs powder was dissolved into 10 mL DMF with stirring for 30 minutes. The sample was measured using a UV-vis spectrophotometer at 480 nm. The concentration of DOX was calculated according to the standard curve of pure DOX/DMF solution. The LC was defined as the weight ratio of loaded DOX to the DOX-loaded NPs. The EE was defined as the weight ratio of loaded DOX to DOX in feed. The LC and EE were calculated according to the equations.

$$LC(\%) = \frac{m_{loaded\ drug}}{m_{drug-loaded\ NPs}} \times 100\%$$

$$EE(\%) = \frac{m_{loaded\ drug}}{m_{drug\ in\ feed}} \times 100\%$$

where $m_{\text{loaded drug}}$ is the amount of loaded DOX in PMs or LPNPs, $m_{\text{drug-loaded NPs}}$ is the total mass of DOX-loaded PMs or DOX-loaded LPNPs, and $m_{\text{drug in feed}}$ is the total mass of DOX when the DOX-loaded PMs or DOX-loaded LPNPs are prepared.

Characterization Of DOX-Loaded NPs

The particle size, size distribution (polydispersity index, PDI), and zeta-potential of blank PMs and LPNPs, DOX-loaded PMs, and DOX-loaded LPNPs was confirmed by dynamic light scattering (DLS) with a Zeta Sizer Nano series Nano-ZS (Malvern Instruments Ltd, Malvern, UK). The sample was prepared at a concentration of 1 mg/mL in a 1.0 mL quartz cuvette and measured using a diode laser of 670 nm with the scattering angle 90° at room temperature.

To study the serum stability, the particle size and PDI of PMs and LPNPs were recorded by DLS after incubation in PBS with 20% FBS for different times (1 day, 2 days, 3 days, and 4 days) at 37°C.

The morphology of the NPs was determined by transmission electron microscopy (TEM, Hitachi H-7650, Japan). Briefly, the sample (1 mg/mL) was dropped onto

the copper grids coated with carbon. The deionized water was removed, and the sample was observed by TEM with an acceleration voltage of 80 kV.

Critical Micelle Concentration (CMC) Measurement

The CMC values of different formulation at different pH values were confirmed by the fluorescence technique using pyrene as the dye according to previous reference with few modifications.[7] Briefly, a series of mixed carrier system solution with concentrations from 0.0001 to 0.1 mg/mL with the pre-prepared pyrene solution (12×10^{-12} M) were prepared as reported.[7] After incubation in dark overnight at room temperature, the samples were recorded with a fluorescence spectrophotometer (F-4500, Hitachi, Japan).

pK_b Measurement

The base dissociation constant (pK_b) of the system was determined using potentiometric titration method. In brief, the PMs or LPNPs with 7% PEGylated lipid was dissolved into deionized water, and the pH of solution was adjusted to 3.5 with diluted HCl, followed by dropwise addition of NaOH (0.1 mol/L) with stirring at room temperature. The real-time pH value was recorded by an automatic titration titrator (Hanon T-860, Jinan, China). The pK_b value was defined as the solution pH at 50% neutralization of tertiary amine groups.[35]

In Vitro Release Of DOX From NPs

The in vitro release profile of DOX from PMs or LPNPs at different pH with or without DTT (used as reducing agent) was studied using dialysis method. In brief, 4 mg DOX-loaded PMs or DOX-loaded LPNPs was dispersed into 4 mL PBS at different pH values (pH 7.4 or 6.5) with or without DTT (10 mM). The solution was moved into a dialysis bag, followed by immersing into corresponding solution (46 mL) in a beaker which was incubated at 37°C with stirring (110 rpm). At pre-determined time intervals, 1 mL solution was collected from the beaker for UV-vis measurement at 480 nm, and 1 mL fresh solution was added. The cumulative DOX release percent (E_r) was calculated according to the following equation.

$$E_r\,(\%) = \frac{V_e \sum_{1}^{n-1} C_i + V_0 C_n}{m_{DOX}} \times 100\,\%$$

where m_{DOX} is the amount of loaded DOX in PMs or LPNPs, V_e is the volume of solution in the dialysis bag (4 mL), V_0 is the total volume of solution in the dialysis bag (4 mL) and beaker (46 mL), and C_i is the concentration of DOX in the ith sample.

Cell Culture

Lewis lung carcinoma (3LL) cells were cultured in high glucose DMEM containing FBS (10%, v/v), sodium pyruvate (1 mM), glutamine (4 mM), HEPES (10 mM), streptomycin (100 μg/mL), and penicillin (100 units/mL). Cells were maintained in a humidified 5% CO_2 incubator at 37°C.

Cellular Uptake Assay

The cellular uptake of LPNPs with a different amount of PEGylated lipid by 3LL cells was evaluated. Briefly, 3LL cells were cultured in 6-well plates with a concentration of 2×10^5 cells/well in DMEM supplemented with the element mentioned above at 37°C. The plates were incubated overnight in a CO_2 (95: 5) incubator. Different LPNPs formulations were added, and incubated for another 2 hours. Then the plates were washed with cold PBS three times. Subsequently, the cells were harvested by trypsin and centrifugation (300 g, 10 minutes). The suspension was removed, and the cells were washed (PBS, 3-times). Finally, the resulting cells were re-suspended in PBS, and analyzed using Accuri C6 flow cytometer (BD Biosciences, San Jose, CA) after filtration through a 100 μm filter.

Cytotoxicity Test

To investigate the biocompatibility and toxic effect of systems, the cytotoxicity of PMs, LPNPS, free DOX, DOX-loaded PMs, and DOX-loaded LPNPs against 3LL cells was evaluated by CCK-8 kits.[36] In brief, 3LL cells were cultured in 96-well plates at a density of 1×10^5 cells/well and cultured for 24 hours in the incubator. The supernatant in each well was removed, and 200 μL of pre-prepared sample was added in every well. The fresh medium was used as a negative control. After incubation for 24 hours, 10 μL of cell counting kit-8 was added in every well. After incubation for 4 hours at 37°C, the absorption at 490 nm was measured by a microplate spectrophotometer (Bio-Rad Laboratories Inc., Hercules, CA), and the cell viability was calculated according to the following formula.

$$Cell\ viability = \frac{A\ sample - A\ blank}{A\ control - A\ blank} \times 100\%$$

where $A_{control}$, A_{sample}, and A_{blank} were the absorbance at 490 nm of well without sample treatment, with sample

treatment, and medium only, respectively. The cytotoxicity test was performed in replicates of six wells.

Statistical Analysis

The experimental data were presented as the mean±standard deviation (SD). Student's *t*-test (Excel, 2007) was used to analyze the data. Statistical significance was considered to be significant when *P*-values were less than 0.05 ($P<0.05$).

Results And Discussion

Optimization Of PEGylated Lipid Modification

The PEGylated lipid was introduced to fabricate hybrid LPNPs with optimized particle size, enhanced drug loading capacity, and improved cellular uptake by tumor cells.[37–39] Therefore, a series of LPNPs with different mole ratios of PEGylated lipid (0%, 3%, 5%, 7%, and 10%) were prepared, the particle size, PDI, and cellular uptake were evaluated carefully. As shown in Figure 2A, the particle size of PMs with 0% of DSPE-mPEG self-assembled from amphiphilic diblock polymer PBAE-ss-mPEG was approximately 120 nm. With the increase of PEGylated lipid, the hydrodynamic diameter of LPNPs was decreased, resulting from the intervention of hydrophobic DSPE segment. When the mole ratio of DSPE-mPEG increased from 0% to 7%, the particle size of LPNPs was reduced from about 120 nm to 80 nm. When the mole ratio of DSPE-mPEG was 10%, the particle size of LPNPs was slightly increased. The reason could be that introduction of PEGylated lipid might facilitate the formation of compact core of LPNPs through self-assembly together with PBAE-ss-mPEG at low mole ratio, while high mole ratio of PEGylated lipid could enhance the size of core due to the aliphatic chain in DSPE segment.[40,41] The uniformity of LPNPs with different mole ratios of PEGylated lipid was evidenced by measurement of PDI, as shown in Figure 2B. All PDIs of LPNPs were reasonably low (<0.30), indicating the good uniformity and homogeneity.[42] Moreover, the CMC values of LPNPs were determined by fluorescence spectroscopy using pyrene as a probe, as shown in Figure S1. The CMC of amphiphilic polymer PBAE-ss-mPEG was 13.4 μg/mL. After PEGylated lipid modification, the CMC was obviously decreased to 9.8 μg/mL because of the introduction of the hydrophobic DSPE segment.[43] Next, the cellular uptake of LPNPs by 3LL cells was evaluated to further investigate the optimization of PEGylated lipid modification, as shown in Figure 2C. The cellular uptake by 3LL cells was significantly enhanced when the mole ratio of PEGylated lipid increased from 0% to 7%, suggesting the physical modification of DSPE-mPEG was able to enhance the internalization of LPNPs by 3LL cells. Furthermore, the percentage of 3LL cells internalized NPs at mole ratio of 10% was similar to that at 7%. Therefore, the fabrication of LPNPs self-assembled from PBAE-ss-mPEG and DSPE-mPEG (93:7, mole ratio) had suitable particle size and exhibited the highest cellular internalization.

To further confirm the optimization of PEGylated lipid modification and evaluate the drug loading capacity of LPNPs, the LC and EE of LPNPs were analyzed, and the results are shown in Tables S1 and 1. With the increase of DOX in feed, the LC of PMs was increased from 5.5% to 11.8%, while the EE of PMs was increased from 36.4% to 40.2% first and then decreased to 34.3% (Table S1). It confirmed that the mass ratio of polymer to DOX in feed of 50:15 was the optimal formulation. Hence, this formulation was used to analyze the drug loading efficiency of LPNPs, and the results were shown in Table 1. As expected, the LC and EE of LPNPs were enhanced markedly in comparison to those of PMs. When the mole ratio of PEGylated lipid increased from 0% to 10%, the LC and

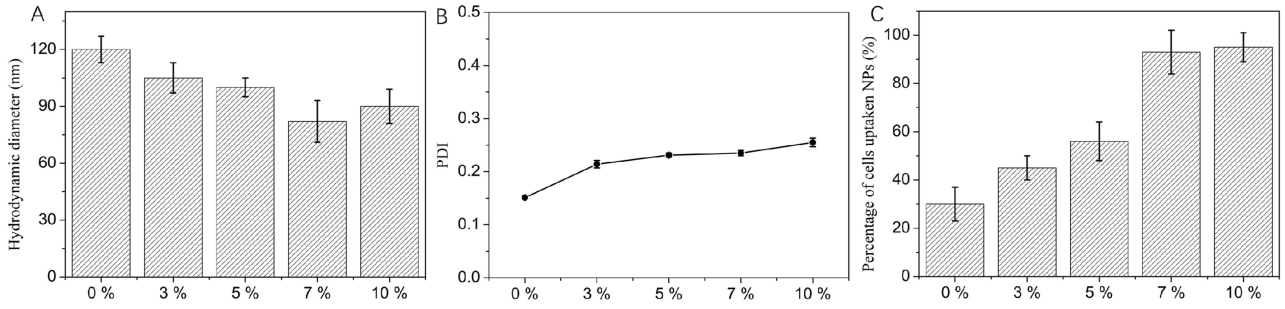

Figure 2 Hydrodynamic diameter (**A**) and polydispersity index (PDI) of LPNPs formulated with a different amount of DSPE-mPEG measured by DLS (n=3, mean±SD). Cellular internalization (**C**) of LPNPs after incubation with 3LL cells for 2 hours determined by flow cytometry.

Table 1 Characteristic Properties Of DOX-Loaded LPNPs

Lipid (%)	LC (%)	EE (%)	Particle Size (nm)	PDI	Zeta-Potential (mV)
0	9.6	40.2	130.7	0.215	−1.5
3	12.3	50.8	112.6	0.243	−2.3
5	14.7	59.7	108.4	0.277	−2.9
7	18.6	76.9	95.3	0.286	−4.1
10	19.5	79.4	105.8	0.334	−5.2

EE were increased from 9.6% to 19.5% and 40.2% to 79.4%, respectively. Specifically, the LC and EE of LPNPs at 7% of PEGylated lipid were 18.6% and 76.9%, respectively. When the mole ratio of DSPE-mPEG increased from 7% to 10%, the LC and EE were slightly increased. Collectedly, the PEGylated lipid modification could effectively enhance the drug loading capacity of LPNPs, and the DOX-loaded LPNPs with 7% of PEGylated lipid would be used for the further study. In addition, for DOX-loaded PMs and DOX-loaded LPNPs, the particle size and PDI were slightly increased compared to the blank PMs and LPNPs, resulting from the encapsulated DOX molecules in the core increasing in size. The zeta-potential of LPNPs was slightly lower than those of PMs because of the modification of DSPE-mPEG.[37]

Serum Stability

To acquire prolonged circulation time and improved accumulation at tumor site *via* EPR effect, the prepared DOX-loaded LPNPs should have high serum stability.[43] Therefore, we next evaluated the serum stability *via* analysis of particle size and PDI of DOX-loaded LPNPs after incubation in PBS (pH 7.4) with 20% FBS at 37°C for different times, as shown in Figure 3. After incubation for 4 days, the particle size of DOX-loaded PMs was increased from about 130 nm to 240 nm, while the particle size of DOX-loaded LPNPs was slightly increased from 95 nm to about 140 nm (Figure 3A). Furthermore, the PDI of DOX-loaded LPNPs showed negligible change in comparison to that of DOX-loaded PMs (from 0.215 to 0.617). These results demonstrated that the DOX-loaded LPNPs with PEGylated lipid modification showed high serum stability compared with DOX-loaded PMs without PEGylated lipid modification, indicating DOX-loaded LPNPs might possess prolonged circulation time in the body.

Stimuli-Responsibility Of LPNPs

The pH/redox-sensitivity of LPNPs was next investigated, as shown in Figures 4 and S2. The pK_b values of polymer PBAE-ss-mPEG and the system of PBAE-ss-MPEG with

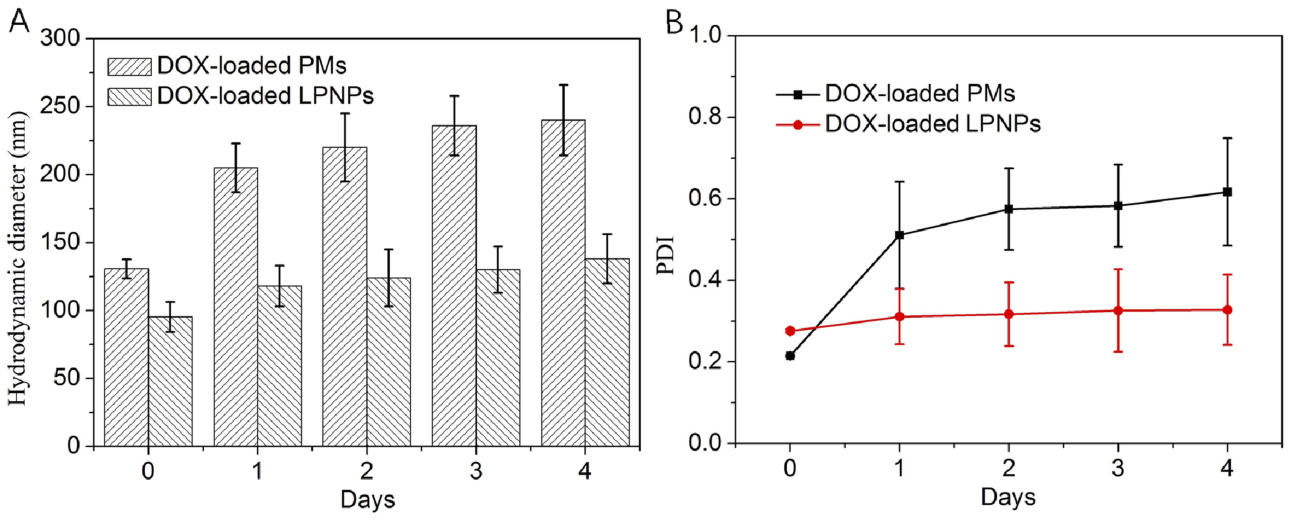

Figure 3 Hydrodynamic diameter (**A**) and polydispersity index (PDI) (**B**) of LPNPs after incubation in PBS (pH 7.4) with 20% FBS at 37°C for different time (n=3, mean ±SD).

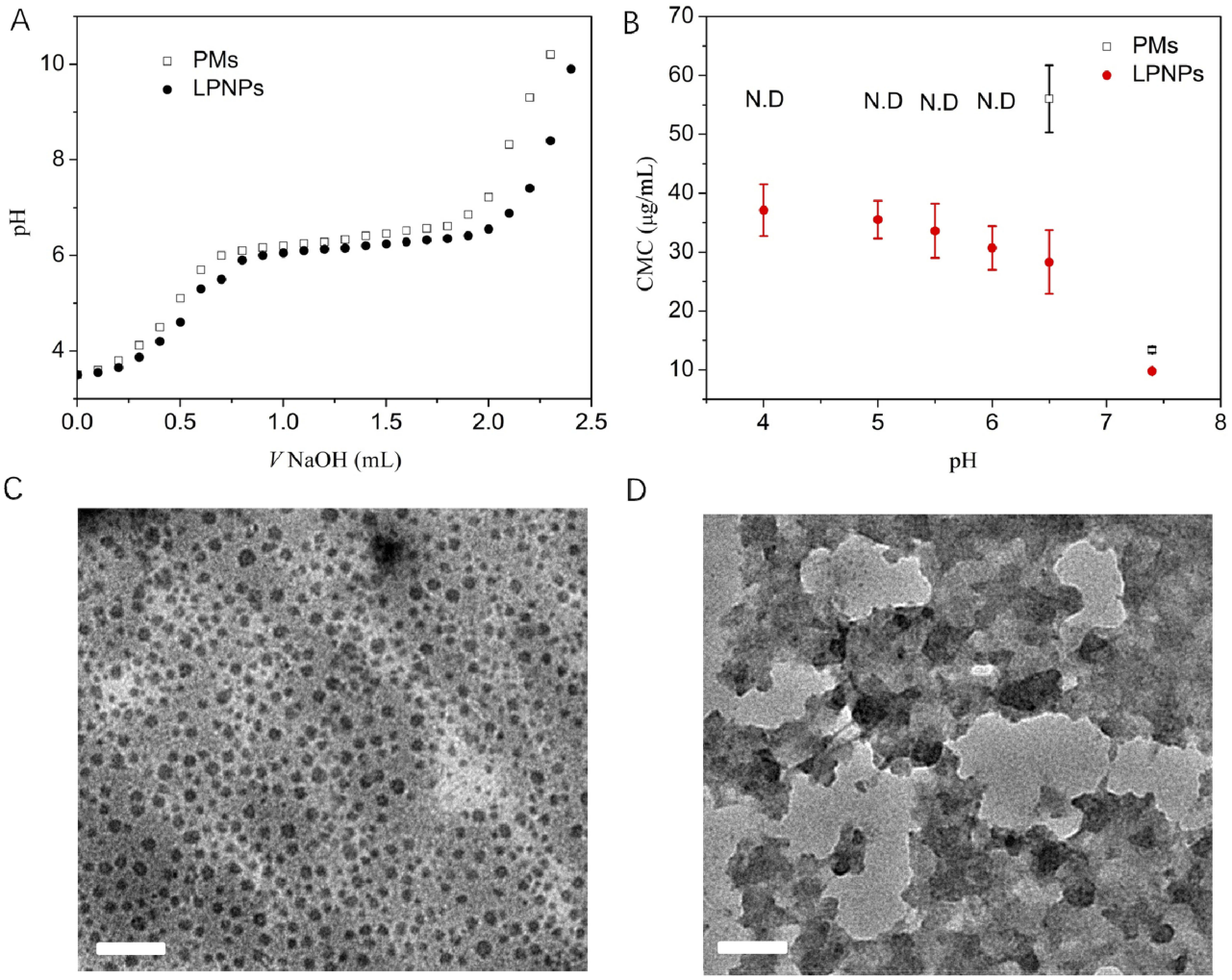

Figure 4 The acid-base titration curve (**A**) of the PMs and LPNPs (7% of DSPE-mPEG, mole ratio) solution. The CMCs (**B**) of PMs and LPNPs (7% of DSPE-mPEG, mole ratio) at different pH values (n=3, mean±SD). TEM images of LPNPs (7% of DSPE-mPEG, mole ratio) after incubation in PBS at pH 7.4 without (**C**) or with (**D**) DTT (10 mM) for 4 hours at 37°C. Scale bar = 500 nm.

7% (mole ratio) of DSPE-mPEG were determined by an acid-base titration, as shown in Figure 4A. Both of them showed a similar change trend with the addition of NaOH solution. At the beginning of titration, the pH value of solution was increased sharply, and then reached a plateau. The reason could be that the tertiary amine residues of PBAE were ionized at weakly acidic condition. With continuous addition of NaOH solution, the pH value was increased rapidly. According to previous report,[22] the pK_b values of polymer PBAE-ss-mPEG and mixed system were determined as 6.51 and 6.55, respectively, indicating the PMs and LPNPs could respond to the weakly acidic cue. To further investigate the pH-sensitivity of LPNPs, the CMC values of PMs and LPNPs at different pH were measured. As shown in Figure 4B, the CMC value of PMs at pH 7.4 was 13.4 μg/mL, while it increased to 56 μg/mL when the pH decreased to 6.5. When the pH decreased to be more acidic (pH<6.0), the CMC of PMs was not detectable, indicating the demicellization of PMs caused by protonation of the tertiary amine residues in PBAE. By contrast, the CMC of LPNPs was increased from 9.8 μg/mL to 37.1 μg/mL when the pH was decreased from 7.4 to 4.0. This result also suggested that LPNPs had much higher stability than that of PMs. Moreover, the zeta-potential of PMs and LPNPs at different pH conditions was measured (Figure S2). When the pH was higher than 7.4, the zeta-potential of PMs and LPNPs was negative due to the shielding effect of PEG shell on the surface of NPs. In a weakly acidic environment, the zeta-potential of PMs and LPNPs was markedly increased with a decrease of pH values because of ionization of tertiary amine residues in the PBAE segment. In summary, these

findings provided the pH-sensitivity of PMs and LPNPs. Figures 4C and D show the morphology of LPNPs after incubation in PBS at pH 7.4 with or without DTT (10 mM) for 4 hours at 37°C. The LPNPs showed spherical morphology with a size of approximately 100 nm in the absence of DTT (Figure 4C). However, the spherical structure was not observed in the presence of DTT, resulting from the cleavage of disulfide bonds which induced aggregation (Figure 4D).[44] These findings demonstrated the redox-responsibility of LPNPs. Summarily, the fabrication of LPNPs could respond to weakacidity and a high concentration of reducing agent.

In Vitro Drug Release Profile

Since the LPNPs showed dual pH/redox-sensitivity, the in vitro DOX release profiles from DOX-loaded PMs and DOX-loaded LPNPs under physiological condition (pH 7.4) with or without DTT (10 mM) and extracellular (pH 6.5) and intracellular (pH 6.5 with 10 mM DDT) conditions were measured using dialysis method. The results are shown in Figure 5. At pH 7.4, less than 30% of DOX (27.1% for DOX-loaded PMs and 23.5% for DOX-loaded LPNPs) was released for 24 hours, indicating the DOX molecules could be protected well in the core of PMs or LPNPs. In Figure 5A, when the pH was decreased to 6.5, the drug release rate from PMs was sharply accelerated due to the protonation of tertiary amine residues in PBAE segment.[7] The cumulative release of DOX was 43.3% and 90.1%, respectively, for 2 hours and 24 hours, indicating the intense initial burst release. At pH 7.4 with 10 mM DTT, the drug release rate was also accelerated in comparison to that at pH 7.4 without DTT, resulting from the cleavage of disulfide bonds. At pH 6.5 with 10 mM DTT, the DOX molecules were released quickly, and the cumulative release was 60.5% and 97.8%, respectively, for 2 hours and 24 hours due to the simultaneous protonation of tertiary amine residues cleavage of disulfides. In Figure 5B, similar drug release profiles could be observed. However, the DOX-loaded LPNPs showed better drug controlled release property in comparison to the DOX-loaded PMs. At pH 6.5, the cumulative release of DOX was 27.5% and 70.4%, respectively, for 2 hours and 24 hours, suggesting the resistant initial burst release and pH-triggered drug release profile. At pH 6.5 with 10 mM DTT, the cumulative release of DOX was 46.8% and 97.5%, respectively, for 2 hours and 24 hours. In addition, weak acidity could trigger the DOX release from PMs and LPNPs when comparing with addition of reducing agent DTT. The reason could be that the protonation of tertiary amine residues could result in the transformation of solubility of PBAE segment from hydrophobicity to hydrophilicity, leading to the demicellization of PMs or swelling of LPNPs with increased porosity. Nevertheless, the cleavage of disulfide bonds could only induce detachment of PEG shell. For DOX-loaded LPNPs, because of PEGylated lipid modification, the DOX molecule was well controlled release from LPNPs with reduced initial burst release compared to that from PMs. In summary, LPNPs modified with DSPE-mPEG showed improved drug release profiles

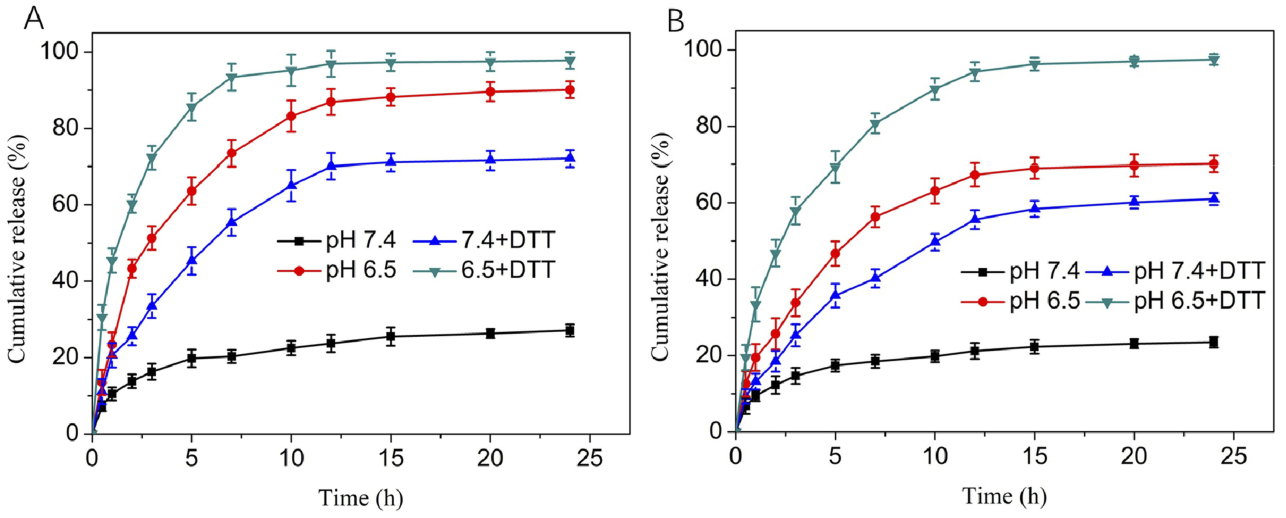

Figure 5 In vitro release profiles of DOX from DOX-loaded PMs (**A**) and DOX-loaded LPNPs (**B**) in PBS at different conditions (pH 7.4, pH 6.5, pH 7.4 with 10 mM DTT, and pH 6.5 with 10 mM DTT) (n=3, mean±SD).

in comparison to PMs and might be potential drug delivery carriers.

Cytotoxicity Test

The biocompatible nano-scale carriers which were expected to be used in clinic should possess low cytotoxicity and capacity of effectively killing the tumor cells.[45] Therefore, the cytotoxicity of blank PMs and fabrication of LPNPs against 3LL cells was evaluated, as shown in Figure 6A. The cytotoxicity of PMs and LPNPs was slightly increased with the increasing of concentration, and the cell viability for the treatment of PMs and LPNPs at the highest concentration (1,000 mg/L) was 80.1% and 90.3%, respectively. Compared to the PMs, the fabrication of LPNPs modified with PEGylated lipid displayed much lower cytotoxicity, indicating higher biocompatibility. Figure 6B showed the toxic effect of free DOX, DOX-loaded PMs, and DOX-loaded LPNPs against 3LL cells for 24 hours. As expected, DOX-loaded LPNPs showed the highest cytotoxicity for 3LL cells due to improved cellular uptake (Figure 2C) and drug release behavior (Figure 5B) in comparison to DOX-loaded PMs. Interestingly, the cytotoxicity of DOX-loaded LPNPs was slightly higher than that of free DOX. The reason could be that the fabrication of LPNPs modified with PEGylated lipid could efficiently deliver DOX molecules into the cytoplasm. In summary, the LPNPs showed negligible cytotoxicity, and the DOX-loaded LPNPs could effectively induce the tumor cells death.

Conclusion

In the present study, biocompatible dual pH/redox-responsive hybrid lipid-polymer nanoparticles (LPNPs) were fabricated using amphiphilic polymer PBAE-ss-mPEG and PEGylated lipid DSPE-mPEG (Figure 1). The drug loading capacity (LC and EE), cellular uptake, and serum stability were significantly enhanced due to the introduction of PEGylated lipid. The hydrodynamic diameter and uniformity of LPNPs were also improved (Figures 2 and 3). These optimized physicochemical properties suggested that the LPNPs fabrication might have prolonged circulation time, enhanced accumulation at the tumor site, and improved internalization by tumor cells, indicating they could efficiently deliver anticancer drug to the targeted site. As shown in Figure 4, the tertiary amine residues in PBAE segment could be protonated at weakly acidic conditions, and the disulfide bonds were cleavable at high concentration of DTT. All findings indicated that the LPNPs fabrication showed pH/redox-sensitivity. The in vitro drug release experiment demonstrated that the DOX molecules could be controlled release from LPNPs in response to the weakacidity and higher concentration of DTT (Figure 5). Moreover, the fabrication of LPNPs displayed lower cytotoxicity in comparison to PMs, and the DOX released from LPNPs could efficiently kill the tumor cells compared to the free DOX (Figure 6). In summary, the LPNPs might be promising anticancer drug delivery carriers with pH and redox-triggered drug release profiles and negligible cytotoxicity. In addition, fabrication of PEGylated lipid and functional polymer could be a useful

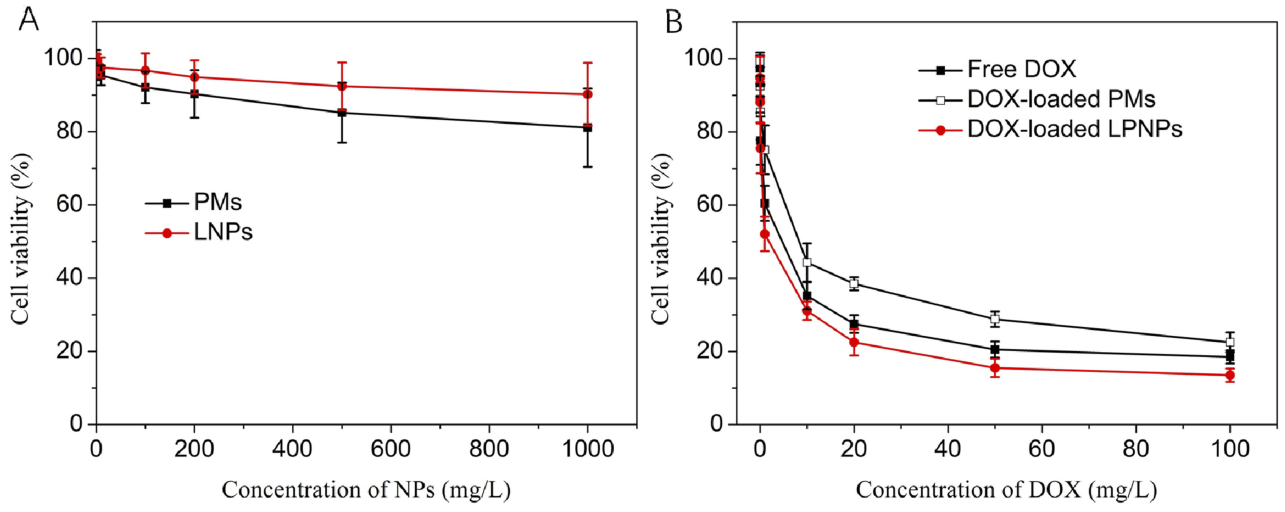

Figure 6 Cell viability of 3LL cells treated with blank PMs and LPNPs (**A**), free DOX, DOX-loaded PMs and DOX-loaded LPNPs (**B**) for 24 hours in concentration specified.

method to prepare a multifunctional platform for drug delivery.

Acknowledgments

This work was financially supported by the Research Foundation of Education Bureau of Liaoning Province, China (Grant No. LK201614). We thank Dr. Sundar Prasanth Authimoolam (Singapore-MIT Alliance for Research and Technology, Singapore) for helping to revise the manuscript.

Disclosure

The authors report no conflicts of interest in this work.

References

1. Ma X, Yu H. Global burden of banker. *Yale J Biol Med*. 2006;79(3–4):85–94.
2. Yang J, Zhang J, Xing J, Shi Z, Han H, Li Q. Inhibition of proliferation and migration of tumor cells through phenylboronic acid-functionalized polyamidoamine-mediated delivery of a therapeutic DNAzyme Dz13. *Inter J Nanomed*. 2019;14:6371–6385. doi:10.2147/IJN.S211744
3. Lucky SS, Idris NM, Huang K, et al. In vivo biocompatibility, biodistribution and therapeutic efficiency of titania coated upconversion nanoparticles for photodynamic therapy of solid oral cancers. *Theranostics*. 2016;6(11):1844–1865. doi:10.7150/thno.15088
4. Chen Z, Zhao P, Luo Z, et al. Cancer cell membrane-biomimetic nanoparticles for homologous-targeting dual-modal imaging and photothermal therapy. *ACS Nano*. 2016;10(11):10049–10057. doi:10.1021/acsnano.6b04695
5. Nagarsheth N, Wicha MS, Zou W. Chemokines in the cancer microenvironment and their relevance in cancer immunotherapy. *Nat Rev Immunol*. 2017;17(9):559–572. doi:10.1038/nri.2017.49
6. Wong SF, Bounthavong M, Nguyen CP, Chen T. Outcome assessments and cost avoidance of an oral chemotherapy management clinic. *J Natl Compr Canc Netw*. 2016;14(3):279–285. doi:10.6004/jnccn.2016.0033
7. Zhang CY, Yang YQ, Huang TX, et al. Self-assembled pH-responsive MPEG-b-(PLA-co-PAE) block copolymer micelles for anticancer drug delivery. *Biomaterials*. 2012;33(26):6273–6283. doi:10.1016/j.biomaterials
8. Saravanakumar G, Kim J, Kim WJ. Reactive-oxygen-species-responsive drug delivery systems: promises and challenges. *Adv Sci*. 2016;4(1):1600124. doi:10.1002/advs.201600124
9. Liu D, Yang F, Xiong F, Gu N. The smart drug delivery system and its clinical potential. *Theranostics*. 2016;6(9):1306–1323. doi:10.7150/thno.14858
10. Dai L, Liu J, Luo Z, Lia M, Cai K. Tumor therapy: targeted drug delivery systems. *J Mater Chem B*. 2016;4:6758–6772. doi:10.1039/C6TB01743F
11. Zhang M, Xu C, Wen L, et al. A hyaluronidase-responsive nanoparticle-based drug delivery system for targeting colon cancer cells. *Cancer Res*. 2016;76(24):7208–7218. doi:10.1158/0008-5472.CAN-16-1681
12. El-Sawy HS, Al-Abd AM, Ahmed TA, El-Say KM, Torchilin VP. Stimuli-responsive nano-architecture drug-delivery systems to solid tumor micromilieu: past, present, and future perspectives. *ACS Nano*. 2018;12(11):10636–10664. doi:10.1021/acsnano.8b06104
13. Yang K, Feng L, Liu Z. Stimuli responsive drug delivery systems based on nano-graphene for cancer therapy. *Adv Drug Deliv Rev*. 2016;105(Pt B):228–241. doi:10.1016/j.addr.2016.05.015
14. Zhang CY, Chen Q, Wu WS, Guo XD, Cai CZ, Zhang LJ. Synthesis and evaluation of cholesterol-grafted PEGylated peptides with pH-triggered property as novel drug carriers for cancer chemotherapy. *Colloids Surf B Biointerfaces*. 2016;142:55–64. doi:10.1016/j.colsurfb
15. Wang X, Yan F, Liu X, et al. Enhanced drug delivery using sonoactivatable liposomes with membrane-embedded porphyrins. *J Control Release*. 2018;286:358–368. doi:10.1016/j.jconrel.2018.07.048
16. Hu K, Zhou H, Liu Y, et al. Hyaluronic acid functional amphipathic and redox-responsive polymer particles for the co-delivery of doxorubicin and cyclopamine to eradicate breast cancer cells and cancer stem cells. *Nanoscale*. 2015;7(18):8607–8618. doi:10.1039/c5nr01084e
17. Schafer FQ, Buettner GR. Redox environment of the cell as viewed through the redox state of the glutathione disulfide/glutathione couple. *Free Radic Biol Med*. 2001;30(11):1191–1212. doi:10.1016/s0891-5849(01)00480-4
18. Balkwill FR, Capasso M, Hagemann T. The tumor microenvironment at a glance. *J Cell Sci*. 2012;125(Pt 23):5591–5596. doi:10.1242/jcs.116392
19. Zhang Y, Peng L, Chu J, et al. pH and redox dual-responsive copolymer micelles with surface charge reversal for co-delivery of all-trans-retinoic acid and paclitaxel for cancer combination chemotherapy. *Int J Nanomedicine*. 2018;13:6499–6515. doi:10.2147/IJN.S179046
20. Xu C, Song RJ, Lu P, et al. pH-triggered charge-reversal and redox-sensitive drug-release polymer micelles codeliver doxorubicin and triptolide for prostate tumor therapy. *Int J Nanomedicine*. 2018;13:7229–7249. doi:10.2147/IJN.S182197
21. Li J, Ma YJ, Wang Y, Chen BZ, Guo XD, Zhang CY. Dual redox/pH-responsive hybrid polymer-lipid composites: synthesis, preparation, characterization and application in drug delivery with enhanced therapeutic efficacy. *Chem Eng J*. 2018;341:450–461. doi:10.1016/j.cej.2018.02.055
22. Zhang CY, Xiong D, Sun Y, Zhao B, Lin WJ, Zhang LJ. Self-assembled micelles based on pH-sensitive PAE-g-MPEG-cholesterol block copolymer for anticancer drug delivery. *Int J Nanomed*. 2014;9:4923–4933. doi:10.2147/IJN.S69493
23. Zhang CY, Gao J, Wang Z. Bioresponsive nanoparticles targeted to infectious microenvironments for sepsis management. *Adv Mater*. 2018;30(43):e1803618. doi:10.1002/adma.201803618
24. Bechler SL, Lynn DM. Characterization of degradable polyelectrolyte multilayers fabricated using DNA and a fluorescently-labeled poly(*β*-amino ester): shedding light on the role of the cationic polymer in promoting surface-mediated gene delivery. *Biomacromolecules*. 2012;13(2):542–552. doi:10.1021/bm2016338
25. Lynn DM, Langer R. Degradable poly (*β*-amino esters): synthesis, characterization, and self-assembly with plasmid DNA. *J Am Chem Soc*. 2000;122(44):10761–10768. doi:10.1021/ja0015388
26. Capasso Palmiero U, Kaczmarek JC, Fenton OS, Anderson DG. Poly (*β*-amino ester)-co-poly(caprolactone) terpolymers as nonviral vectors for mRNA delivery in vitro and in vivo. *Adv Healthc Mater*. 2018;7(14):e1800249. doi:10.1002/adhm.201800249
27. Tu Y, Peng F, White PB, Wilson DA. Redox-sensitive stomatocyte nanomotors: destruction and drug release in the presence of glutathione. *Angew Chem Int Ed Engl*. 2017;56(26):7620–7624. doi:10.1002/anie.201703276
28. Xu M, Zhang CY, Wu J, et al. PEG-detachable polymeric micelles self-assembled from amphiphilic copolymers for tumor-acidity-triggered drug delivery and controlled release. *ACS Appl Mater Interfaces*. 2019;11(6):5701–5713. doi:10.1021/acsami.8b13059
29. Fang Y, Xue J, Gao S, et al. Cleavable PEGylation: a strategy for overcoming the "PEG dilemma" in efficient drug delivery. *Drug Deliv*. 2017;24(sup1):22–32. doi:10.1080/10717544.2017.1388451

30. van Vlerken LE, Vyas TK, Amiji MM. Poly(ethylene glycol)-modified nanocarriers for tumor-targeted and intracellular delivery. *Pharm Res*. 2007;24(8):1405–1414. doi:10.1007/s11095-007-9284-6
31. Shen Z, Ye H, Kröger M, Li Y. Aggregation of polyethylene glycol polymers suppresses receptor-mediated endocytosis of PEGylated liposomes. *Nanoscale*. 2018;10:4545–4560. doi:10.1039/C7NR09011K
32. Pal K, Madamsetty VS, Dutta SK, Mukhopadhyay D. Co-delivery of everolimus and vinorelbine via a tumor-targeted liposomal formulation inhibits tumor growth and metastasis in RCC. *Int J Nanomed*. 2019;14:5109–5123. doi:10.2147/IJN.S204221
33. Shenoy D, Little S, Langer R, Amiji M. Poly(ethylene oxide)-modified poly(β-amino ester) nanoparticles as a pH-sensitive system for tumor-targeted delivery of hydrophobic drugs: part I. in vitro evaluations. *Mol Pharm*. 2005;2:357–366. doi:10.1021/mp0500420
34. Fang C, Bhattarai N, Sun C, Zhang M. Functionalized nanoparticles with long-term stability in biological media. *Small*. 2009;5:1637–1641. doi:10.1002/smll.200801647
35. Hu YQ, Kim MS, Kim BS, Lee DS. RAFT synthesis of amphiphilic (A-ran-B)-b-C diblock copolymers with tunable pH-sensitivity. *J Polym Sci Pol Chem*. 2008;46(11):3740–3748. doi:10.1002/pola.22717
36. Wang H, Gu W, Xiao N, Ye L, Xu Q. Chlorotoxin-conjugated graphene oxide for targeted delivery of an anticancer drug. *Int J Nanomed*. 2014;9:1433–1442. doi:10.2147/IJN.S58783
37. Liu X, Xiang J, Zhu D, et al. Fusogenic reactive oxygen species triggered charge-reversal vector for effective gene delivery. *Adv Mater*. 2016;28(9):1743–1752. doi:10.1002/adma.201504288
38. Wong HL, Bendayan R, Rauth AM, Xue HY, Babakhanian K, Wu XY. A mechanistic study of enhanced doxorubicin uptake and retention in multidrug resistant breast cancer cells using a polymer-lipid hybrid nanoparticle system. J. *Pharmacol Exp Ther*. 2006;317(3):1372–1381. doi:10.1124/jpet.106.101154
39. Kaczmarek JC, Patel AK, Kauffman KJ, et al. Polymer-lipid nanoparticles for systemic delivery of mRNA to the lungs. *Angew Chem Int Ed Engl*. 2016;55(44):13808–13812. doi:10.1002/anie.201608450
40. Hervella P, Alonso-Sande M, Ledo F, Lucero ML, Alonso MJ, Garcia-Fuentes M. PEGylated lipid nanocapsules with improved drug encapsulation and controlled release properties. *Curr Top Med Chem*. 2014;14(9):1115–1123. doi:10.2174/1568026614666140329224716
41. Stepniewski M, Pasenkiewicz-Gierula M, Róg T, et al. Study of PEGylated lipid layers as a model for PEGylated liposome surfaces: molecular dynamics simulation and langmuir monolayer studies. *Langmuir*. 2011;27:7788–7798. doi:10.1021/la200003n
42. Poon Z, Chang D, Zhao X, Hammond PT. Layer-by-layer nanoparticles with a pH-sheddable layer for in vivo targeting of tumor hypoxia. *ACS Nano*. 2011;5:4284–4292. doi:10.1021/nn200876f
43. Jung SH, Kim SK, Jung SH, et al. Increased stability in plasma and enhanced cellular uptake of thermally denatured albumin-coated liposomes. *Colloids Surf B Biointerfaces*. 2010;76:434–440. doi:10.1016/j.colsurfb.2009.12.002
44. Yang L, Fang W, Ye Y, Wang Z, Hu Q, Tang BZ. Redox-responsive fluorescent AIE bioconjugate with aggregation enhanced retention features for targeted imaging reinforcement and selective suppression of cancer cells. *Mater Chem Front*. 2019;3:1335–1340. doi:10.1039/C9QM00216B
45. Mura S, Nicolas J, Couvreur P. Stimuli-responsive nanocarriers for drug delivery. *Nat Mater*. 2013;12:991–1003. doi:10.1038/nmat3776